

**SECTION**

**THE JOHNS HOPKINS UNIVERSITY**  
DEPARTMENT OF AERONAUTICS  
BALTIMORE 18 MARYLAND  
Operating Under Contract NOrd 8036  
With the Bureau of Ordnance, U. S. Navy

AD 634781

# HEAT LOSS OF HOT-WIRES IN SUPERSONIC FLOW

by  
**Leslie S. G. Kováshay**  
and  
**Sven I. A. Törmärck**

|  |            |          |
|--|------------|----------|
| CLEARINGHOUSE<br>FOR FEDERAL SCIENTIFIC AND<br>TECHNICAL INFORMATION |            |          |
| Hardcopy   | Microfiche |          |
| \$2.00   | \$1.50     | 34 pp. a |
| <b>ARCHIVE COPY COPY</b>   |            |          |



D D C  
RECEIVED  
JUL 7 1966  
RECEIVED  
B

**Bumblebee Series**  
**Report No. 127**  
**Copy No. 270**

**April 1950**

DISTRIBUTION OF THIS  
DOCUMENT IS UNLIMITED

# HEAT LOSS of HOT WIRES in SUPERSONIC FLOW

by

LESLIE S. G. KOVÁSZNAY

and

SVEN I. A. TÖRMARCK



THE JOHNS HOPKINS UNIVERSITY

DEPARTMENT OF AERONAUTICS

BALTIMORE, MARYLAND.

**BLANK PAGE**

## TABLE OF CONTENTS

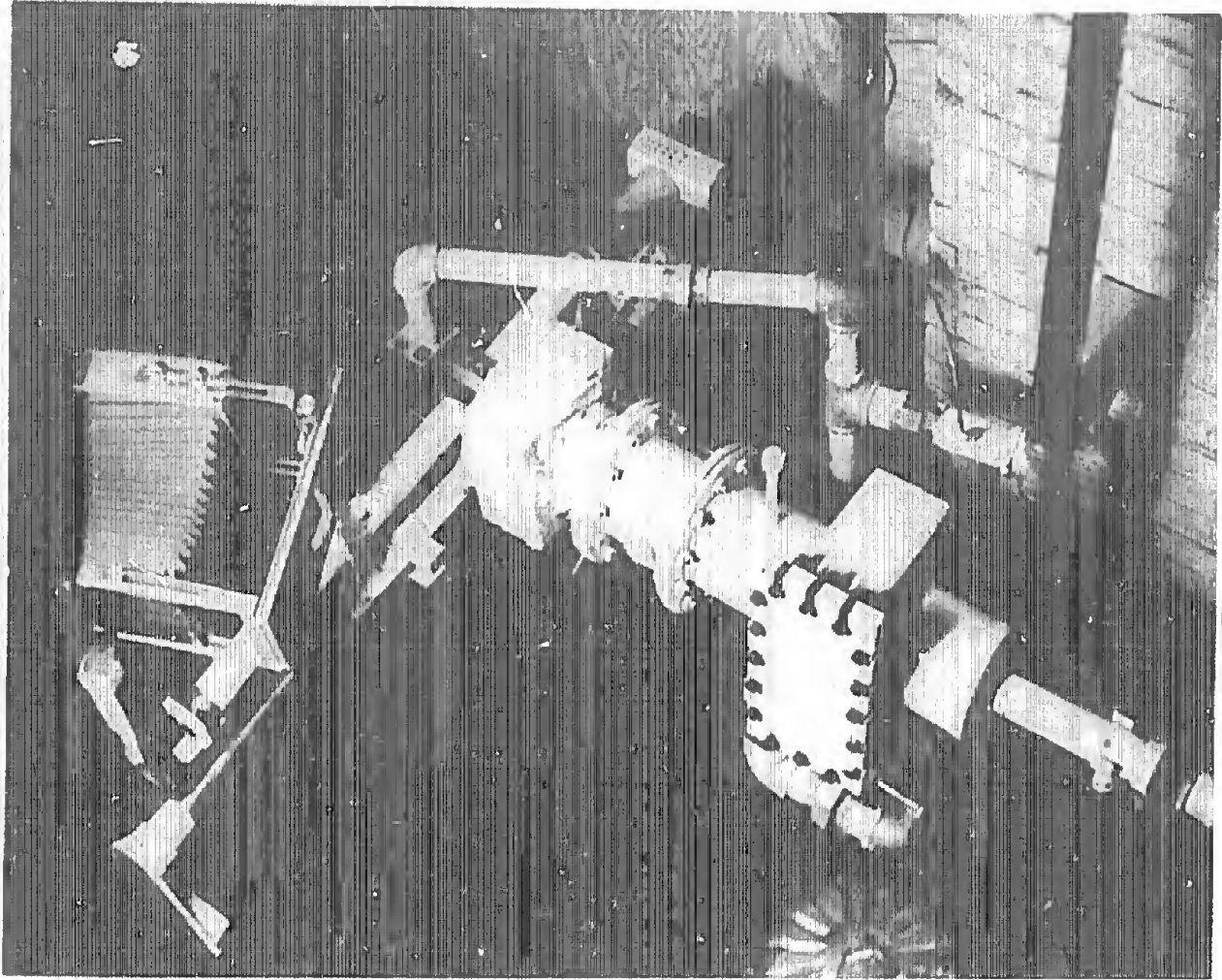
|   |    |
|---|----|
| INTRODUCTION . . . . .                    | 1  |
| WIRES . . . . .                           | 1  |
| ELECTRICAL CIRCUIT . . . . .              | 5  |
| CALIBRATING FACILITY . . . . .            | 5  |
| DATA REPRESENTATION . . . . .             | 10 |
| EXPERIMENTAL DATA . . . . .               | 15 |
| COMPARISON WITH EXISTING THEORY . . . . . | 25 |
| CONCLUDING REMARKS . . . . .              | 26 |
| NOTATION . . . . .                        | 27 |

## LIST OF ILLUSTRATIONS

| <u>Fig. No.</u>  | <u>Page No.</u> |
|--|-----------------|
| Frontispiece   | iv              |
| 1. Electron Microscope Pictures of Tungsten Wires . . . . .                      | 4               |
| 2. Method of Mounting Hot-Wires . . . . .  | 4               |
| 3. Temperature Coefficient of Resistivity for Wire . . . . .                     | 6               |
| 4. Electrical Circuit . . . . .  | 6               |
| 5. Schematic Diagram of the Calibrating Facility . . . . .                       | 8               |
| 6. Supersonic Calibrating Facility . . . . .                                     | 8               |
| 7. Supersonic Nozzle With Schlieren Equipment Removed . . .                      | 9               |
| 8. Hot-Wire Holder at Various Mach Numbers . . . . .                             | 9               |
| 9. Determination of Mach Number . . . . .  | 11              |
| 10. End Loss Correction . . . . .  | 13              |
| 11. Equilibrium Temperature of Hot-Wire in<br>Supersonic Flow . . . . .          | 18              |
| 12. Heat Loss in Wire at Supersonic Speeds.<br>Wire Diameter 0.0003 in. . . . .  | 18              |
| 13. Heat Loss in Wire at Supersonic Speeds.<br>Wire Diameter 0.00015 in. . . . . | 19              |
| 14. Heat Loss in Wire at Supersonic Speeds.<br>Wire Diameter 0.0003 in. . . . .  | 19              |
| 15. Heat Loss in Wire at Supersonic Speeds.<br>Wire Diameter 0.00015 in. . . . . | 21              |
| 16. Heat Loss of Wire at Supersonic Speeds.<br>- Large and Small Wire . . . . .  | 22              |
| 17. Heat Loss vs Temperature Loading . . . . .                                   | 24              |

### ACKNOWLEDGEMENT

The authors are greatly indebted to Mr. P. Iribe and Miss P. Clarcken for their help with experiments and photographic work, and to Dr. F. H. Clauser for his interest and constructive criticism.



**CALIBRATING EQUIPMENT FOR HOT-WIRE STUDIES**

## INTRODUCTION

The application of the hot-wire anemometer to supersonic flow has had several obstacles, such as inadequate frequency response and difficulty of interpretation, but perhaps the most fundamental information lacking was knowledge of the heat transfer properties of a wire placed in a supersonic flow.

In the low speed application of the hot-wire anemometer the heat loss formula of L. V. King<sup>1</sup> gave an adequate representation of at least the functional relationship between flow parameters and heat loss, even if the numerical constants found by King are not of much practical use. King's formula establishes a linear relationship between the Nusselt number and the square root of Reynolds number. The Nusselt number seems to be essentially independent of the temperature difference, indicating a linear dependence of heat loss on temperature difference.

The hot-wire anemometer has proven to be almost a unique tool in turbulence research although it is not an excellent instrument for measuring mean velocities in the higher velocity ranges. Its usefulness stems from its relatively small inertia and from the fact that this small inertia can be compensated by appropriate electronic circuits.

The use of hot-wires as turbulence measuring instruments calls for extremely thin wires in order to reduce the thermal lag. These thin wires operate at Reynolds numbers of the order of 10 - 1000. The wire diameter and mean free path are comparable, and at supersonic speeds, for example, the shock wave itself is no longer a relative "discontinuity". The flow around a hot-wire under operation in a supersonic flow is definitely a slip flow in most practical cases.

## WIRES

Keeping in mind that the goal of this investigation was to gain information permitting use of the hot-wires at supersonic speed, we have chosen only wire materials that give satisfactory

---

<sup>1</sup>"On the Convection of Heat from Small Cylinders in a Stream of Fluid", L. V. King, Phil. Trans., of Roy. Soc. A Vol. 214, 1914.

sensitivity. It can be shown from the wire response equation<sup>2</sup> that the fluctuation sensitivity of the hot-wire anemometer is proportional to approximately the 3/2-power of the "overheating ratio":

$$a_w = \alpha (T_w - T_e)$$

where

- $\alpha$  = temperature coefficient of electrical resistivity
- $T_w$  = wire temperature
- $T_e$  = unheated wire temperature (equilibrium temperature).

This fact calls either for a high temperature coefficient of resistivity, a high operating temperature, or both.

Pure metals have high temperature coefficients of resistivity, while alloys have much lower coefficients. On the other hand, most noncorroding metals (platinum, gold, etc.) have low tensile strength. It can be proved that the fluctuation sensitivity of a wire increases proportionately to the length-diameter ratio but, unfortunately, the tensile stress increases the same way. This gives a certain "figure of merit" on hot-wire materials.<sup>3</sup>

$$\text{"Figure of Merit"} = \alpha^{3/2} (T_w - T_e)_{\max}^{3/2} r^{1/2} \sigma_T$$

where

- $\sigma_T$  is the maximum tensile stress
- $r$  specific electric resistivity of the wire

The wire material that has proven to be superior to others up to the present time is tungsten. The two disadvantages of tungsten (it oxidizes at moderate temperatures and it cannot be soft-soldered) are more than balanced by its high strength and good temperature coefficient of resistivity. Platinum-iridium and similar alloys have low temperature coefficients, but may be useful at elevated temperatures.

Tungsten does not permit the use of the Wollaston process but can be bare drawn down to .00030-in. diameter (7.6 microns). Commercial .00015-in. diameter (3.8 microns) wire (made

---

<sup>2</sup> Refer to Equation (12) in "Calibration and Measurement in Turbulence Research by the Hot-Wire Method", L.S.G. Kovásznay, (Translation) NACA Tech. Mem. 1130, June 1947.

<sup>3</sup> Figure of merit is evaluated with the maximum permissible  $l/d$  ratio derived from maximum permissible stress. It becomes apparent that the absolute diameter is not a significant parameter for static sensitivity.

by an etching process) can be obtained; commercial attempts have been made to produce 0.00010-in. (2.5 microns) wires, but with only moderate success, since the wires become uneven and break when handled. The use of the 0.00015-in. wire proved to be practicable. Since its diameter is only seven times the wave-length of yellow light, no optical observation can give much information about surface conditions, uniformity, etc.

Electron microscope pictures have been made of several samples of tungsten wire at the Department of Medicine of The Johns Hopkins University by Dr. J. Murphy. Figure 1 shows samples of both the larger (0.00030 in.) and the smaller (0.00015 in.) wire. The diameter ratio as determined from the picture is close to 1:2, as the nominal diameters would indicate, and the surface conditions are surprisingly good. The smaller wire is gold plated in order to improve its resistance to corrosion and to help the bond between tungsten and copper plating.

Unfortunately the electron microscope used did not permit absolute measurement<sup>4</sup> since its magnification is varied by adjusting the focal length of the electron lens, in contrast to ordinary optical microscopes in which the focusing is done by adjusting the position of the lens.

The wires are mounted by first copper plating the ends and then soft-soldering them to the prongs. This process is extensively described by Schubauer and Klebanoff.<sup>5</sup> The proper design of the hot-wire holder is a more critical problem in supersonic than in low-speed operation. Most wire failures occurred because of dust particles hitting the wires, vibration of the prongs, or fatigue at the end of the wires when operated in a violently fluctuating flow region.

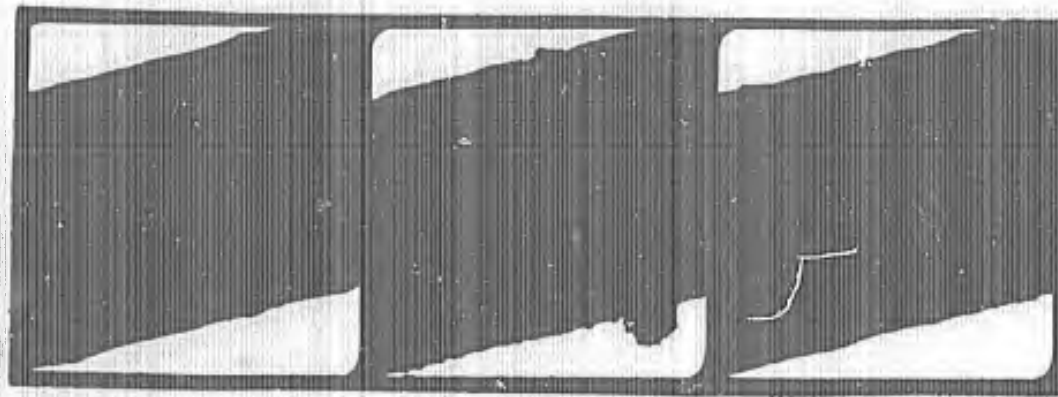
The mounting used in the present experiments is shown in Fig. 2. The prongs are plain sewing needles insulated by an insulating paint and imbedded in a steel wedge. The insulating paint is sufficient since the maximum potential across the wire is only a few volts. The tungsten wires are electro-plated with copper to approximately double diameter and then soft-soldered to the prongs. The copper-plated section protects the ends of the wire from the obliquely intersecting detached shock wave at Mach numbers higher than 1.1.

The length of the uncoated portion of the wire was measured by a travelling microscope

---

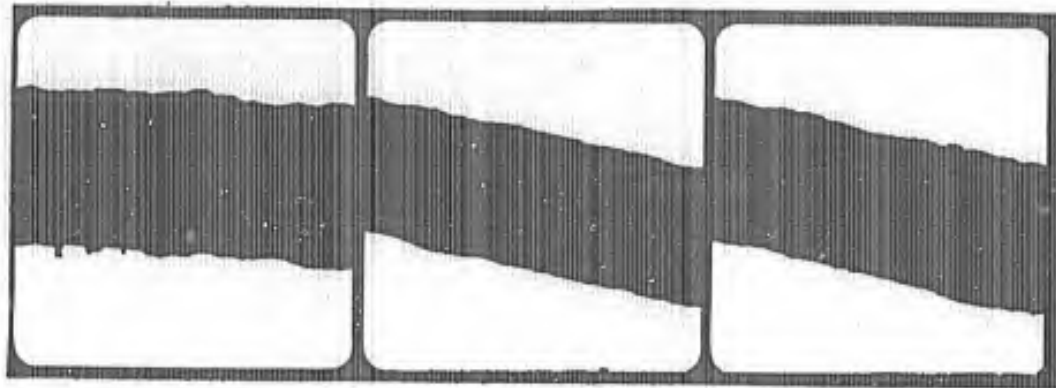
<sup>4</sup> The scale given in Fig. 1 is merely approximate.

<sup>5</sup> "Theory and Application of Hot-Wire Instruments in the Investigation of Turbulent Boundary Layer," Schubauer and Klebanoff, NACA Wartime Report, WO 86, 1946.



TUNGSTEN WIRE 0.0003 inch dia.

1/1000 Inch



TUNGSTEN WIRE GOLD PLATED 0.00015 inch dia.

Fig. 1 ELECTRON MICROSCOPE PICTURES OF TUNGSTEN WIRES

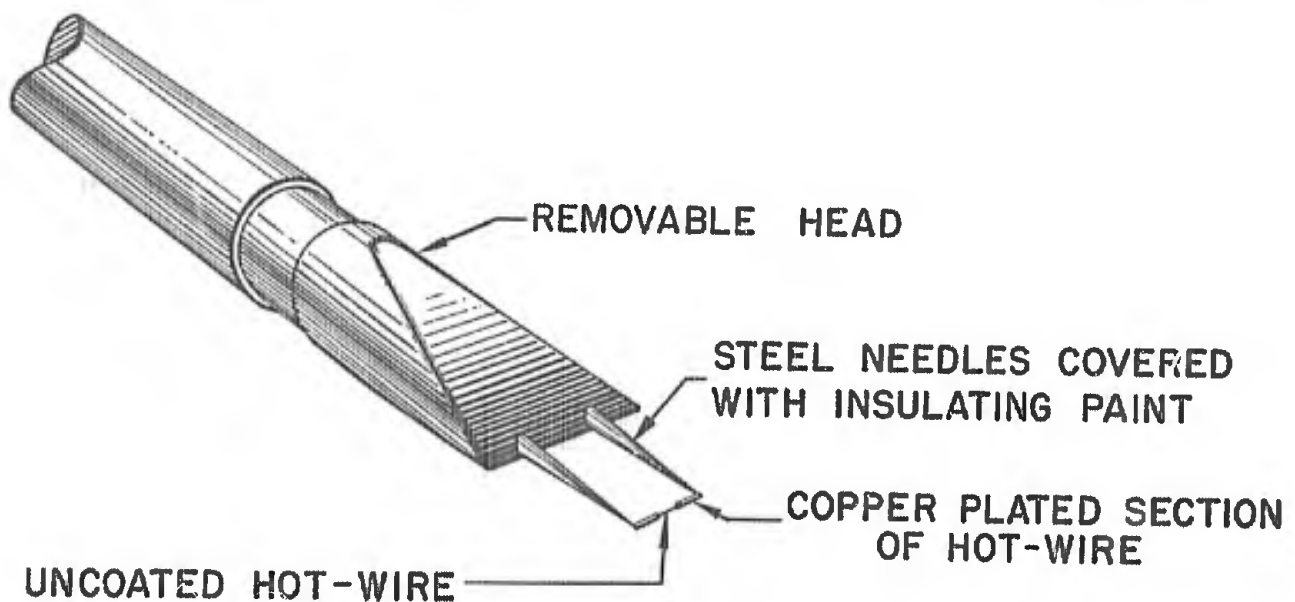


Fig. 2 METHOD OF MOUNTING HOT-WIRES

(comparator) and the uniformity of the wire was estimated from the scattering of data on electrical resistance per unit length of all samples obtained from the same spool. The temperature coefficient of resistivity was measured by cycling a wire sample in a thermostatic oven. The results are given in Fig. 3. The results showed a consistently smaller value than that found in tables for pure tungsten. The smaller wire (0.00015 in.) was gold plated and this may explain its lower value of  $\alpha$ . The curves are essentially linear, although the observed slight nonlinearity has been taken into account in evaluating the heat loss data.

#### ELECTRICAL CIRCUIT

The electrical circuit used is shown in Fig. 4. The circuit consists of two basic parts: a resistance measuring instrument (Wheatstone Bridge) and a heating current measuring instrument (d-c potentiometer). Both parts of the circuit are of conventional type. The wire resistances obtained were in the range of 2 to 30 ohms, and the heating currents in the range 0 to 400 ma.

The sequence of operation usually started with the determination of the "cold resistance" of the wire with no airflow. This was also measured after every supersonic run in a small auxiliary low-speed jet at room temperature by using a very small heating current (1 to 2 ma) and by making corrections for it.

In the supersonic flow the "cold resistance" was measured again. This now corresponded to the equilibrium temperature in the flow. When the wire was heated, the resistance was balanced in the bridge and the heating current was measured with the d-c potentiometer (by determining the d-c voltage drop across the standard resistor. Under slightly drifting flow conditions (stagnation pressure slowly varying in wind tunnel), the readings were taken as the bridge balance galvanometer, G, passed through zero. The accuracy obtained in resistance was approximately 0.01 ohms, or at least 0.05 per cent (whichever is the greater), and the error in heating-current measurement was about 0.1 per cent.

#### CALIBRATING FACILITY

It was realized early in the research that the pioneer series of measurements of hot-wire heat loss in supersonic flow would involve a long and detailed investigation of comparable flexibility. Since one of the main issues involved was connected with Mach number effects, it was imperative that both Reynolds and Mach numbers be varied independently over a sufficient range.

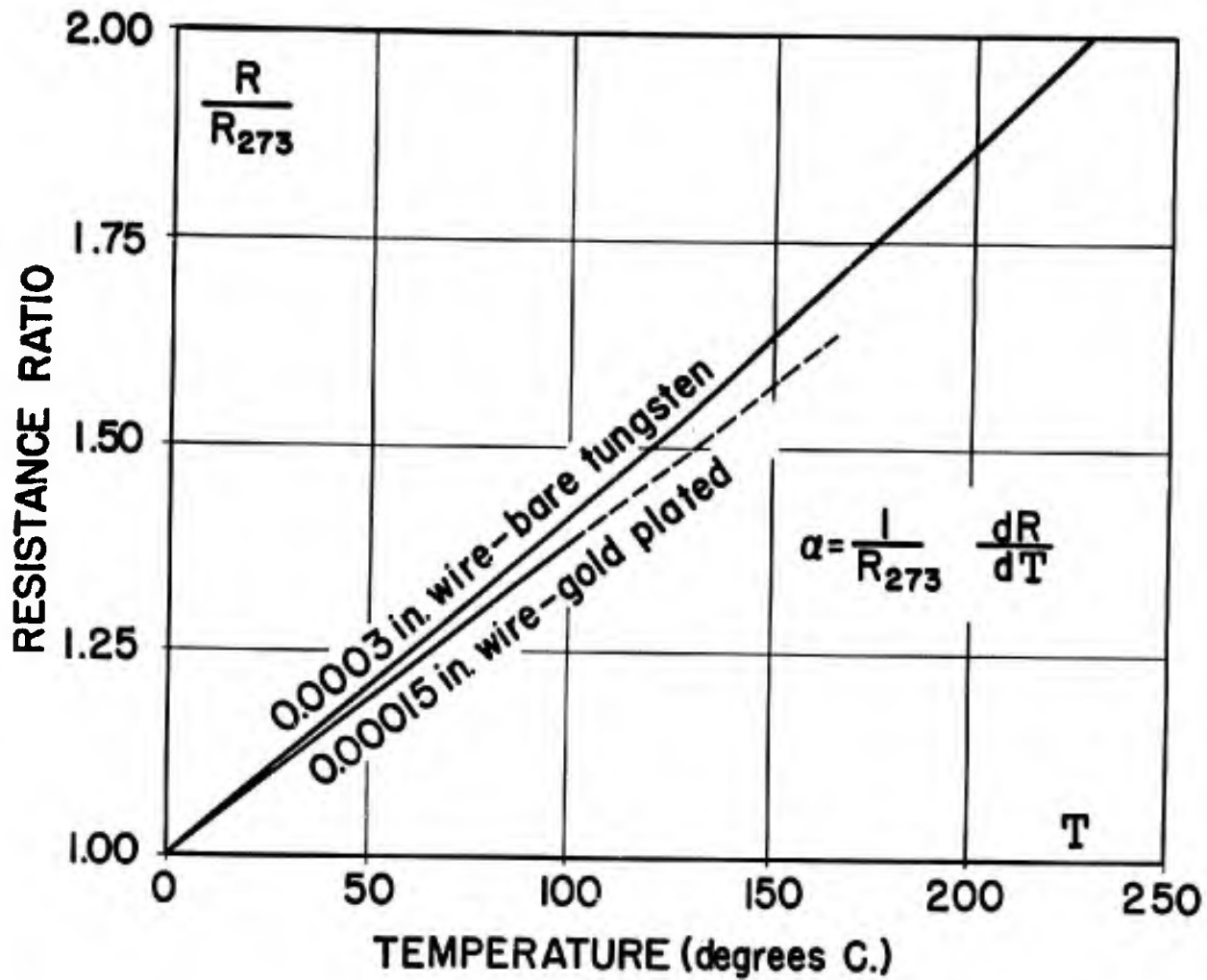


Fig. 3 TEMPERATURE COEFFICIENT OF RESISTIVITY FOR WIRE

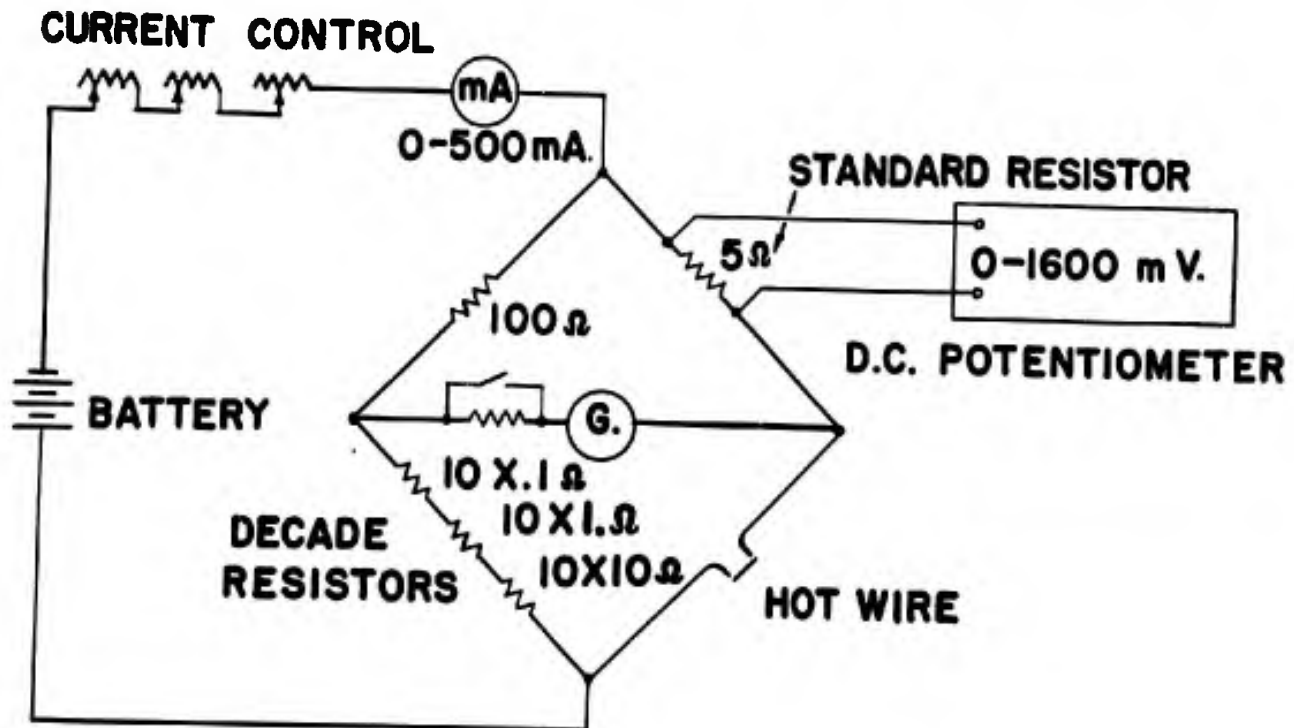


Fig. 4 ELECTRICAL CIRCUIT

Since all existing major supersonic wind tunnels have been quite busy, and since their flexibility is limited, we were forced to build a small calibrating facility just for this type of investigation.

The schematic diagram of the system is shown in Fig. 5.

The working section operates between two large storage tanks, one being a pressure tank and the other a vacuum tank. The pressure difference is maintained by a water-cooled reciprocating compressor which is driven by a 30-hp electric motor. As the air delivered by a compressor normally contains oil, oil vapor, water vapor, and dust, extra filters are installed in the air supply line to the pressure tank. In addition to the standard oil filter, there is an activated-carbon oil filter and a silica gel dryer. Most of the dust particles settle down in the pressure tank. From the pressure tank, the air passes through cotton- and glass-wool filters in order to remove the smaller particles of lint and any remaining dust from the silica gel.

The working section is designed to accommodate hot-wire probes. With several turbulence damping screens and a large contraction, it is believed that the flow is without significant turbulence (the damping screens are operating below their critical Reynolds number). The transonic and supersonic part of the nozzle is rather unconventional. The flow is separated into two separate branches by the wedge shaped hot-wire holder, and the hot-wire holder can be traversed freely between the two "legs" so that the wire can be operated continuously at various Mach numbers without modifying the flow ahead of the wedge. The whole working section part is shown with schlieren bench in Fig. 6.

The working section alone is shown in Fig. 7, and flow pictures at varying Mach numbers are shown in Fig. 8. The needles produce very weak conically-shaped shocks that do not interfere with the uncoated (sensitive) portion of the wire. On the other hand, the strong shock caused by the wedge is always behind the wire as long as the Mach number is above 1.05.

The ambient pressure level in the whole system can be varied in the ratio 1:4 for all except wire Mach numbers higher than 1.6. (The necessary pressure ratio across the working section increases when the wedge is pulled back to produce higher Mach numbers at the wire.) The stagnation temperature was measured in the settling chamber by a mercury thermometer with an accuracy of 1/10 degree centigrade. The stagnation pressure was measured by a mercury manometer with an accuracy of 1 mm of mercury. The stagnation temperature was above atmospheric in the majority of the experiments. Since the working section is very small

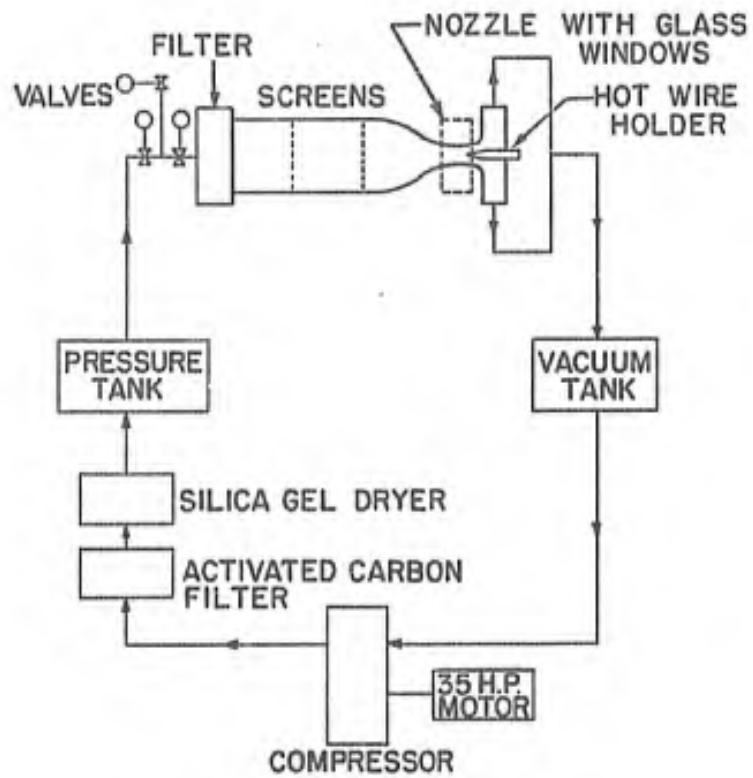


Fig. 5 SCHEMATIC DIAGRAM OF THE CALIBRATING FACILITY

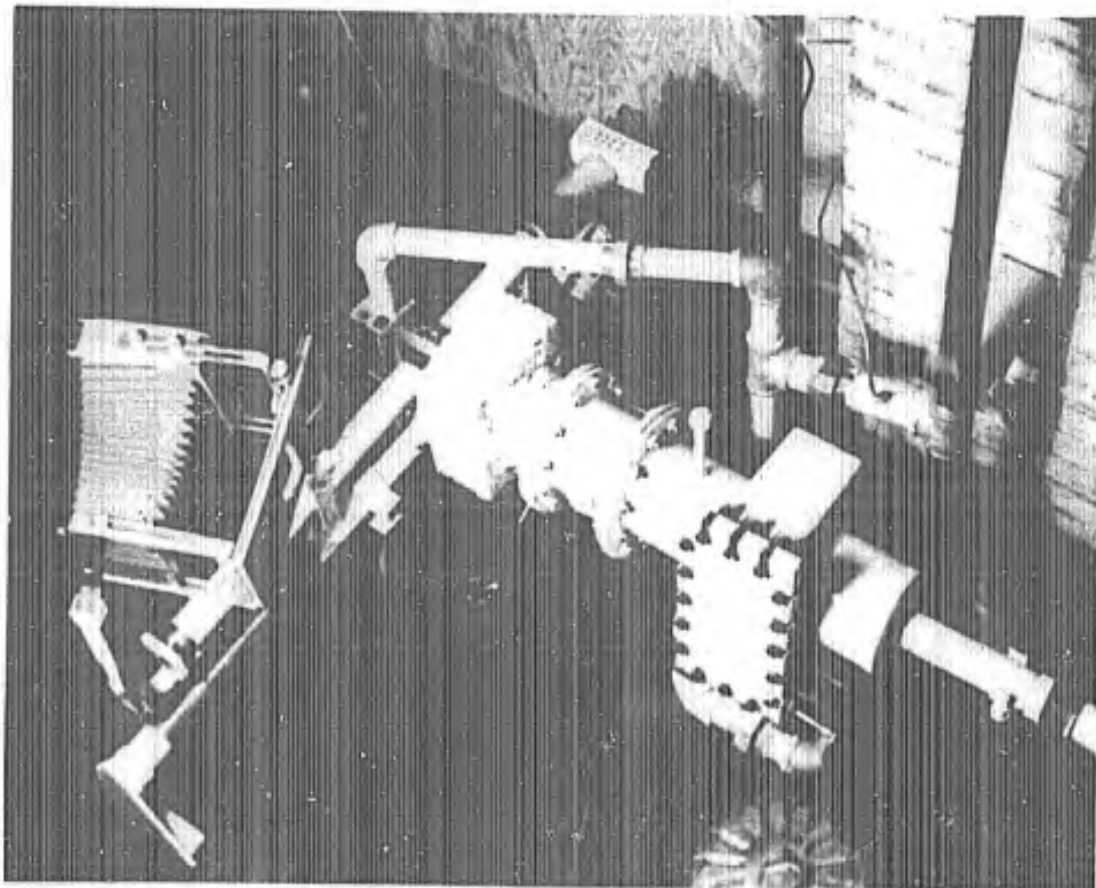


Fig. 6 SUPERSONIC CALIBRATING FACILITY

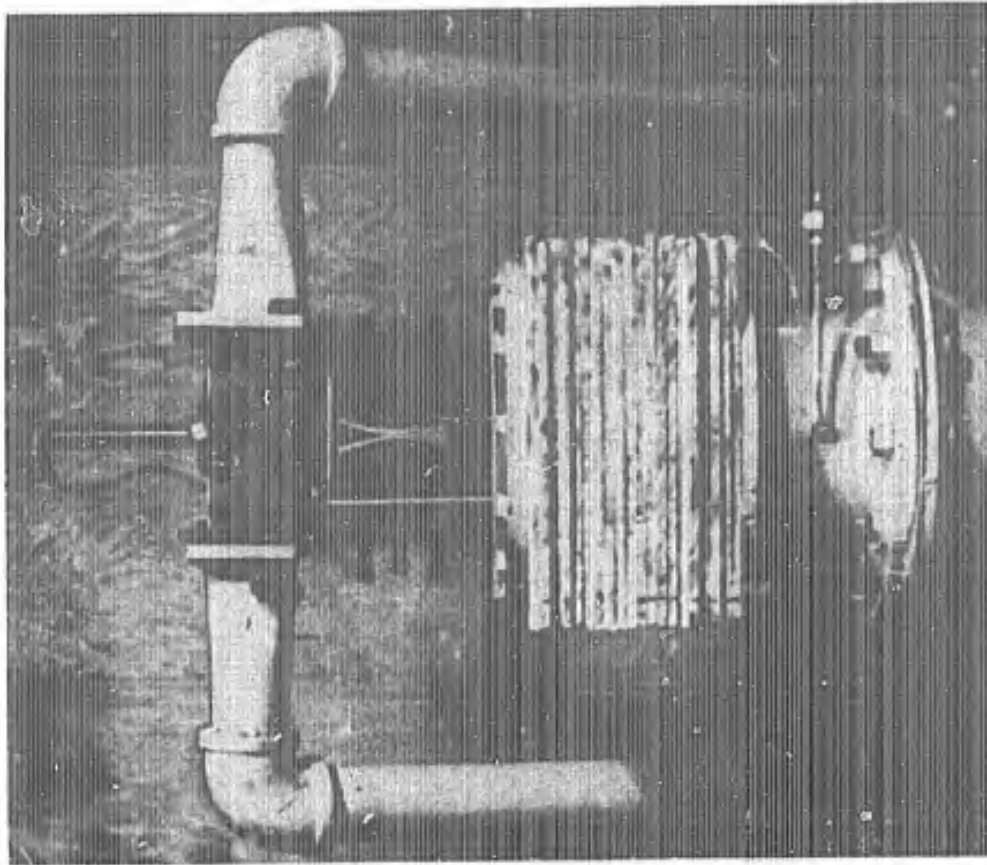


Fig. 7 SUPERSONIC NOZZLE WITH SCHLIEREN EQUIPMENT REMOVED

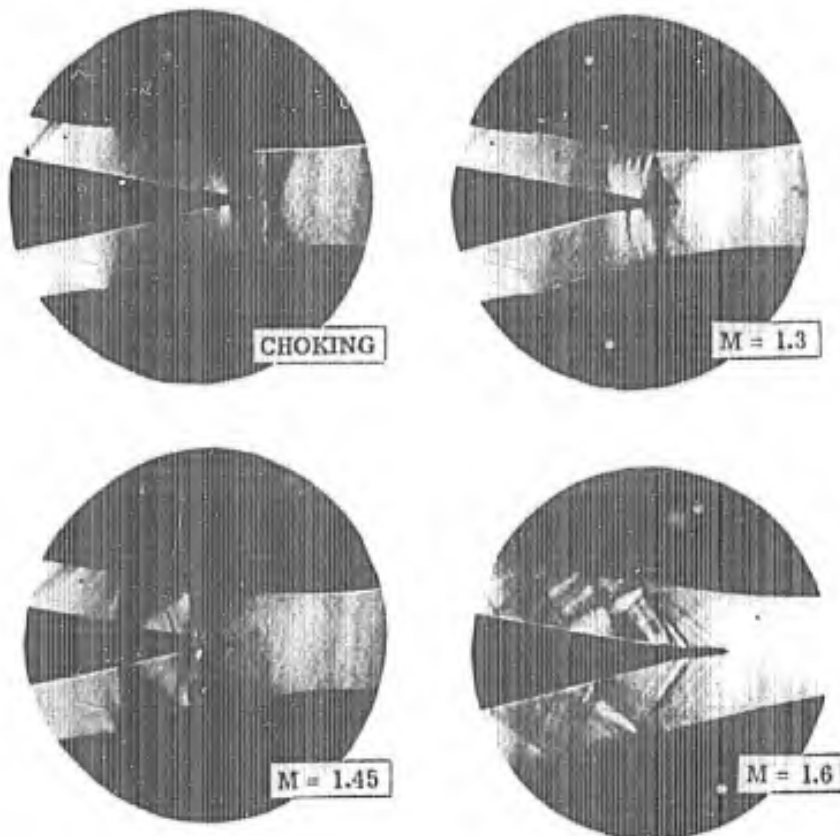


Fig. 8 HOT-WIRE HOLDERS AT VARIOUS MACH NUMBERS

(0.4 x 0.5-in. throat) it can not be "surveyed", and the flow quality was checked only by optical observations.

When the tunnel was first run, separation frequently occurred in one "leg" and most of the flow followed one side of the supersonic section (Coanda effect). After the shock waves were fixed in both "legs", this "flashback" separation was eliminated and a very steady and regular flow field was obtained.

The local Mach number was determined optically from the angle of the Mach waves. In order to make Mach waves more prominent, the top and bottom walls were scratched. The angle determination was obtained from enlarged schlieren pictures as shown in Fig. 9. The accuracy of this determination is estimated to be 2 to 3 per cent in the range of Mach numbers from 1.1 to 2.05.

The schlieren pictures were taken with a short duration spark (3 to 4 microseconds), and repeated exposures proved that the flow was steady and reproducible within the accuracy mentioned.

#### DATA REPRESENTATION

The problem of heat loss from a wire in a viscous compressible flow, where the mean free path is not vanishingly small compared to the body dimensions, presents great difficulty from the theoretical point of view. The only real guidance is offered by dimensional reasoning. If we assume that the heat loss is a function of all pertinent variables,

$$H = H ( U, \rho, p, T_{\text{air}}, T_w, d, \ell, \mu, k, C_p, \tau )$$

The number of variables is rather large. In non-dimensional representation the heat loss is described by the Nusselt number,

$$\text{Nu} = \frac{H}{\pi \ell \Delta T k}$$

and the functional relationship becomes, for perfect gases,

$$\text{Nu} = \text{Nu} ( \text{Re}, M, \text{Pr}, \gamma, \tau, d/\ell )$$

Using air at conventional temperatures, we may assume that  $\text{Pr} = \text{const.}$  and  $\gamma = \text{const.}$ ;  $d/\ell$  in all practical applications is very small since the wires are long compared to their diameter. In this case, the heat loss through the ends can be estimated with reasonable accuracy, as will be shown later. Consequently, data can be corrected to infinitely long wires, just as

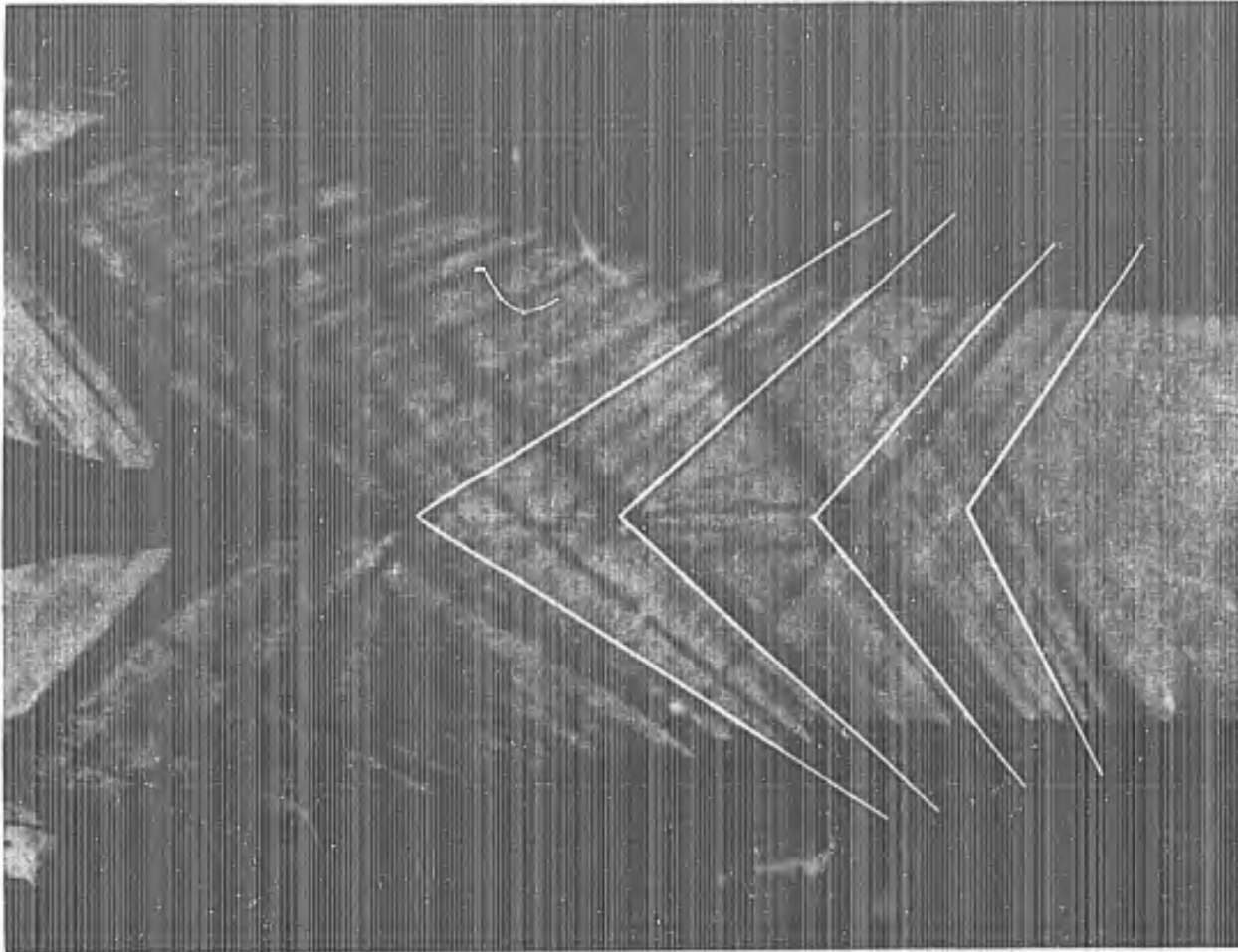


**Fig. 9 DETERMINATION OF MACH NUMBERS**

airplane wing data is reduced to infinite aspect ratio. The temperature loading  $\tau$  is defined as

$$\tau = \frac{\Delta T}{T_0} = \frac{T_w - T_e}{T_0}$$

where temperature difference between wire and surrounding air (equilibrium temperature) is expressed as a fraction of stagnation temperature. The temperature loading expresses the increase in enthalpy of the streamlines passing around the wire and it is a good measure of the distortion in the flow around the wire caused by heat addition.

If the temperature loading is small ( $\tau \rightarrow 0$ ) the heat loss can be expressed as

$Nu = Nu (Re, M, d/L)$ , and for wires which are long in comparison to their diameter, the "end loss" can be computed and corrected for.

The heat propagation along the wire for steady cases was computed by L. V. King<sup>6</sup>, and the result shows the temperature distribution along the span to be a hyperbolic cosine, assuming that the heat loss is proportional to temperature difference. A more elaborate case, including nonlinearity with the readjustment of distribution, was worked out by R. Betchov<sup>7</sup>.

For our purposes the simple linear method is sufficient. After a re-writing of the problem into non-dimensional variables, the resulting transcendent equation was solved numerically.

Denoting:

- $\bar{a}_w$  mean measured overheating ratio  $\bar{a}_w = \alpha ( \bar{T}_w - \bar{T}_e )$
- $a_w^*$  ideal overheating ratio that would occur with infinitely long wire
- $H_{corr.}$  correct value of heat loss
- $H_{meas.}$  measured value of heat loss
- $Nu_{O\ corr.} = \frac{H_{corr.}}{\pi l \Delta T \lambda_o}$  corrected value of Nusselt number (for an infinitely long wire)
- $Nu_{O\ meas.} = \frac{H_{meas.}}{\pi l \Delta T \lambda_o}$  measured Nusselt number
- $K$  heat conductivity of the wire
- $\lambda_o$  heat conductivity of air at stagnation temperature

The end loss correction given by this equation dependent on a non-dimensional parameter

$$S = \frac{d}{l} \frac{\sqrt{1 + \bar{a}_w}}{\sqrt{Nu_{O}}} \sqrt{\frac{K}{\lambda_o}} \quad (1)$$

The functional relationship is given in Fig. 10.

$$\frac{\bar{a}_w}{a_w^*} = f(S)$$

The correction is

$$\frac{H_{corr.}}{H_{meas.}} = \frac{Nu_{O\ corr.}}{Nu_{O\ meas.}} = \frac{\bar{a}_w}{a_w^*} \frac{1 + a_w^*}{1 + \bar{a}_w}$$

Tungsten has almost 4:1 ratio higher heat conductivity than platinum, resulting in a 2:1 ratio in  $S$  and corresponding end-loss effect.

<sup>6</sup> King. op. cit.

<sup>7</sup> "Theorie Non-Lineaire de L' Anemometre a fil chaud," R. Betchov, Proc. of the Royal Dutch Academy of Sciences, Vol. LII, No. 3, 1949.

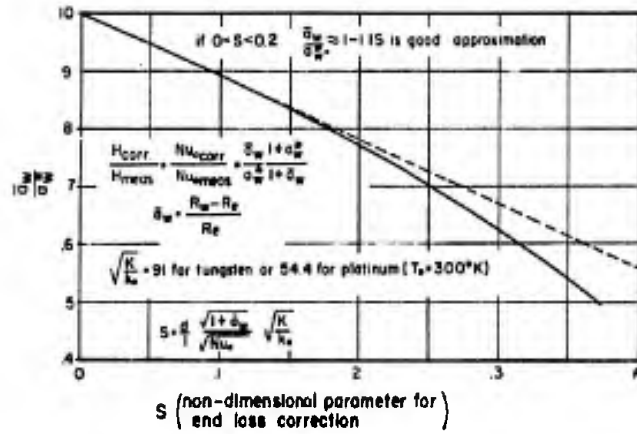


**Fig. 10 END LOSS CORRECTION**

An example with realistic operating conditions:

$$\begin{array}{ll}
 d = .00015 \text{ in.} & \alpha = .0035/\text{centigrade} \\
 \ell = .045 \text{ in.} & T_o = 300^\circ\text{K} \\
 \sqrt{\frac{K}{k_e}} = 91 \text{ tungsten (300}^\circ\text{K)} & \bar{T}_e = 290^\circ\text{K} \\
 \Delta T = 143^\circ \text{ C} & \bar{T}_w = 433^\circ\text{K} \\
 \bar{a}_w = 0.5 & Nu_o = 9.0
 \end{array}$$

This results in the following computed value of end loss correction:

$$S = 0.124 \quad \frac{\bar{a}_w}{a_w^*} = 0.865 \quad \frac{Nu_o \text{ corr.}}{Nu_o \text{ meas.}} = 0.91$$

This means that the end loss of 9 per cent of the total heat loss.

The implicit formula for the end loss based on the heat loss formula of King<sup>8</sup> is

$$\frac{\bar{a}_w}{a_w^*} = 1 - S \sqrt{\frac{a_w^*}{\bar{a}_w}} \tanh \frac{1}{S} \sqrt{\frac{\bar{a}_w}{a_w^*}} \quad (2)$$

The end loss correction is not too important in an actual turbulence measurement, since the sensitivity is expressed with actual operating point parameters; however, in the determination of the general heat loss law it must be taken into account.

For small temperature loading and infinitely long wire (that is  $\tau \rightarrow 0$ ,  $d/\ell \rightarrow 0$ ), the only two significant parameters are the Reynolds number and the Mach number. The important question then arises as to where the flow parameters should be evaluated in order to give the most representative data. Quite obviously the type of "Mach number effect" primarily depends on this question. Prior exploratory measurements (H.L. Dryden and G.B. Schubauer, unpublished)

<sup>8</sup> King, op. cit.

indicated that the heat loss seems to be proportional to the square root of the mass flow  $\rho U$  for a fixed Mach number. (Mach number was not varied in these experiments.)

From the preliminary measurements it became apparent that the Mach number was a secondary parameter when compared to Reynolds number. There is little doubt about the definition of Mach number to be used.

$$M = \frac{U_1}{c_1} \quad \text{where}$$

$U_1$       velocity at free stream condition before the wire  
 $c_1$       speed of sound at free stream conditions.

The Nusselt number contains only one quantity that may depend on the choice of flow parameter, that is,  $k$ , the heat conductivity of the gas.

The Reynolds number contains velocity, density, and viscosity in addition to diameter. The viscosity and heat conductivity are proportional to each other as long as the Prandtl number is constant and within the range in which we were interested. They can be approximated by the power law<sup>9</sup>

$$\frac{k}{k_r} = \frac{\mu}{\mu_r} = \left( \frac{T}{T_r} \right)^{.768} \quad (3)$$

where the subscript r refers to Reference temperature. The other subscripts have the following significance:

- 0 for stagnation conditions
- 1 free stream conditions
- 2 free stream conditions behind normal shock
- e equilibrium temperature
- w wire temperature

The viscosity and heat conductivity can be evaluated under various conditions:

|         |       |
|---------|-------|
| $\mu_0$ | $k_0$ |
| $\mu_1$ | $k_1$ |
| $\mu_2$ | $k_2$ |
| $\mu_e$ | $k_e$ |
| $\mu_w$ | $k_w$ |

---

<sup>9</sup> "Chemical Engineer's Handbook," John H. Perry, McGraw-Hill Co, 1941

or some odd combination thereof. The velocity can be chosen from among

$$U_1, U_2, c_1, c_2, c_0, c^* ;$$

with the knowledge of  $M$  we can always transfer one into the other. The density depends on both temperature and pressure so we may choose any of the above temperatures and one of the pressures  $p_0, p_1, p_2, p_{20}$ .

$p_{20}$  (stagnation pressure behind normal shock)

The conditions behind normal shock are included because it was felt intuitively that the front part of the cylinder, where most of the heat transfer takes place, is in a region behind the almost normal detached shock. The importance of the physical condition of the medium behind a normal shock seems to have been confirmed by some preliminary data communicated by Mr. H. Lowell of Lewis Flight Propulsion Laboratory of the NACA. This variety of conditions permits a great number of choices for the physical variables. The majority can be ruled out on the basis of physical unsoundness.

It was seen, however, that the "Mach number effect" depended essentially on the choice of flow parameters used in forming the Reynolds and Nusselt numbers. This fact suggested the possibility of eliminating the "Mach number effect" completely and using flow parameters which would collapse all data at different Mach numbers into a single plot.

#### EXPERIMENTAL DATA

The experimental data taken consist of three groups: Equilibrium temperature measurements, heat-loss measurements at low temperature loadings, and heat-loss measurements at high temperature loadings. In principle, the parameters can be varied in any manner, but practical considerations made certain organization of effort imperative.

The supersonic calibrating facility operated steadily under one pressure level and drifted slightly toward that pressure level if operated off this value. This meant that the steady state was preferable for operation extended in time, such as accurate determination of equilibrium temperature and the majority of high temperature loading measurements. The Mach number can be changed rather easily merely by changing the position of the wire.

One schlieren picture was taken with every run, and every time doubt arose about the smoothness of flow or change of Mach number, another picture was taken. This meant that

several hundred pictures were taken in the course of the work.

The heat loss at low temperature loading required variation of Reynolds number as the primary variable; therefore the pressure level was varied. The usual procedure was as follows: the pressure level was first set at a maximum (maximum  $Re$ ) and was then dropped down in steps to steady-state operation. All the meters were read at the same time to check out the slow drift.

Unfortunately, both the carbon oil filter and the silica gel filter became saturated after a few hours of operation and required replacement. Dust, small lint particles, or tufts often became attached to the wire. All these difficulties were minimized by using a regular preventive routine during the investigation.

The wire was checked for cold resistance, without mechanical strain, in a low-speed calibrating jet immediately before and after every run. If the two values differed by more than a few hundredths of an ohm, the data was rejected. Dirt particles, especially lint, often lodged on the wire and increased drag to such an extent that the wire was permanently strained. In such cases, it was found that the cold resistance of the wire after the run was increased substantially. If a wire had been overstrained or oxidized (both results are apparent in an increased cold resistance) it usually broke during the next run. Later, when experience had been accumulated, it was possible to predict wire failures from the drift of resistance at room temperature. A resistance decrease after a run never occurred.

During the measuring process any one of the following three parameters was used as primary variable:

1. Position of the wire (Mach number), with fixed heating current and fixed pressure.
2. Pressure in the system (essentially Reynolds number), wire position fixed, wire temperature fixed.
3. Temperature of the wire (temperature loading) with fixed position and tunnel pressure.

Case 1 was used mainly with unheated wires to determine the equilibrium temperature, Case 2 was used for low temperature-loading heat-loss data. In this case, two or three schlieren pictures were taken during a single run and the equilibrium temperature was also checked between every two points in the heat-loss measurements. In Case 3, the variation of heat loss with temperature loading was determined. It was a rather critical operation due to the high wire temperatures; casualties were relatively frequent.

The Case 2 measurements indicated as a by-product that the equilibrium temperature  $T_e$  does not depend on Reynolds number for the larger (.00030") wire, and increases only very slightly with decreasing Reynolds number for the small (.00015") wire. This latter variation was only 1 to 1.5 degrees centigrade and not very systematic. This indicated that the primary parameter for  $T_e$  is Mach number and the results are plotted in Fig. 11. The somewhat higher values for the smaller wires may be the result of surface conditions (the small wire being gold plated) in this slip flow region. No evidence of the "strain-gage effect" was found; the only (slight) change obtained with the smaller wire was in the reverse direction. If a strain-gage effect were present, the wire resistance and the apparent equilibrium temperature would increase with increased air load, or, in other words, with increased Reynolds number.

The result of the measurements, as indicated in Fig. 11, is that the equilibrium temperature is piece-wise constant and rather close to the stagnation temperature.

The heat loss for small temperature loading is given by the Nusselt number, and the primary variable, as stated above, is the Reynolds number, with the Mach number as a secondary parameter. From the numerous combinations of flow parameters, we could plot many different representations. After experimentation with a few combinations, it became apparent that combinations involving conditions at heated wire temperature,  $T_w$ , should be ruled out. It seemed sensible also to keep only combinations in which all physical parameters are evaluated at the same conditions. These considerations left the following choices:

$$\begin{array}{ll}
 0. & Re_0 = \frac{c_0 \rho_0 d}{\mu_0} & Nu_0 = \frac{H}{L \pi \Delta T \epsilon_0} \\
 1. & Re_1 = \frac{U_1 \rho_1 d}{\mu_1} & Nu_1 = \frac{H}{L \pi \Delta T \epsilon_1} \\
 2. & Re_2 = \frac{U_2 \rho_2 d}{\mu_2} & Nu_2 = \frac{H}{L \pi \Delta T \epsilon_2}
 \end{array}$$

The data are plotted in this manner in Fig. 12 and 13. The collapse was quite remarkable although some systematic Mach number effect is still detectable. This effect, however, does not exceed the standard deviation of the data.

The results are not surprising in view of the fact that the Mach number behind the normal shock varies very little compared to the variation of the Mach number before the shock.

The results shown in Fig. 12 and 13 suggest that the heat loss is governed by the subsonic part of the flow field and that the situation is relatively unaffected by wide variations

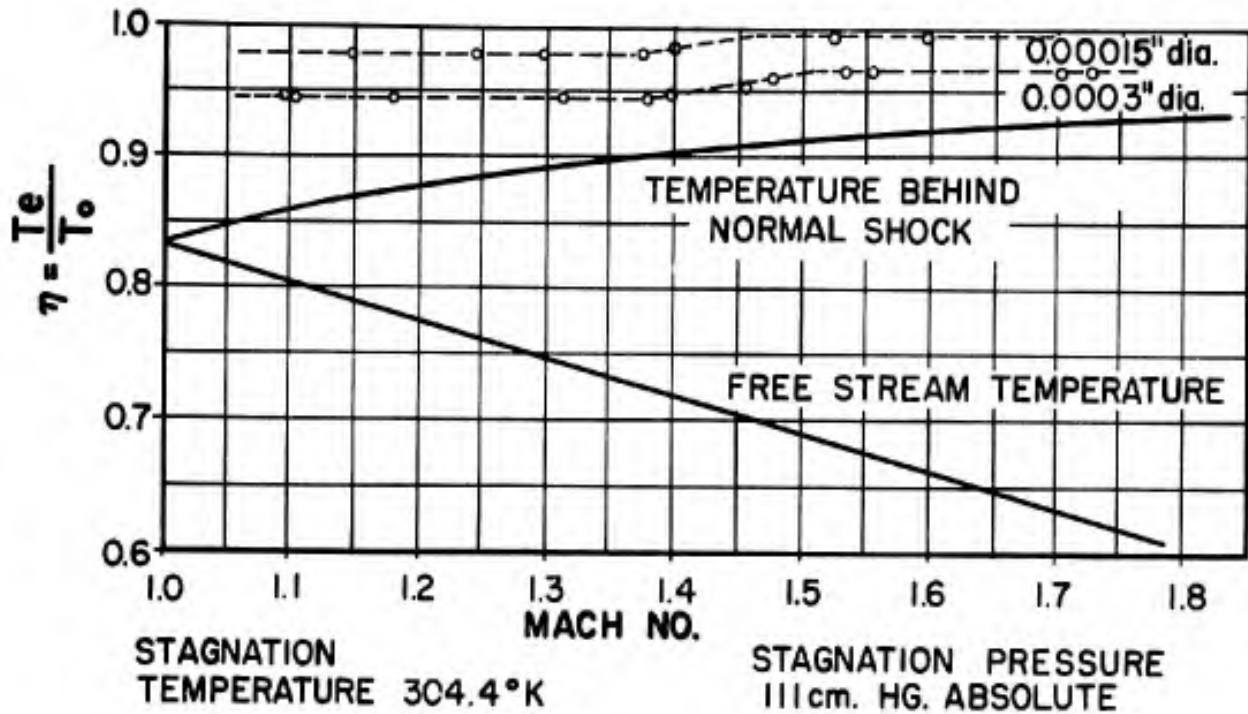


Fig. 11 EQUILIBRIUM TEMPERATURE OF HOT-WIRE IN SUPERSONIC FLOW

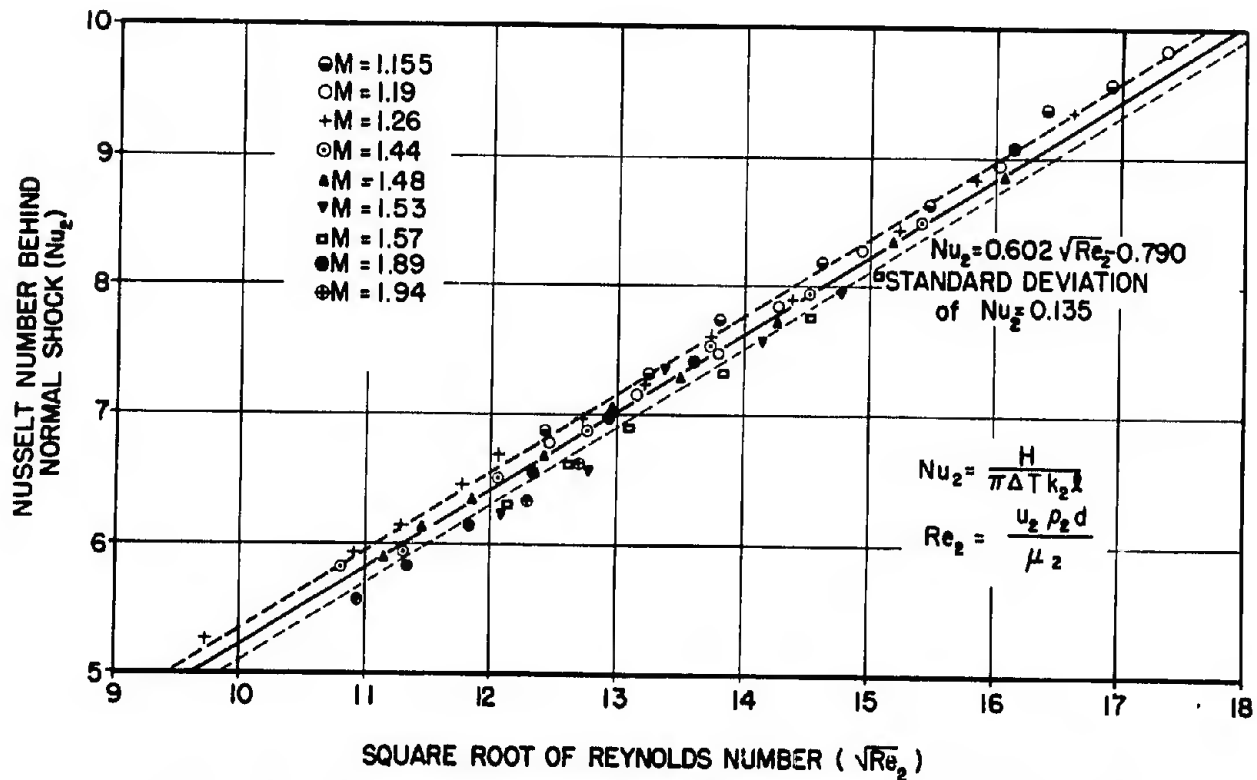


Fig. 12 HEAT LOSS IN WIRE AT SUPERSONIC SPEEDS WIRE DIAMETER 0.0003 INCH

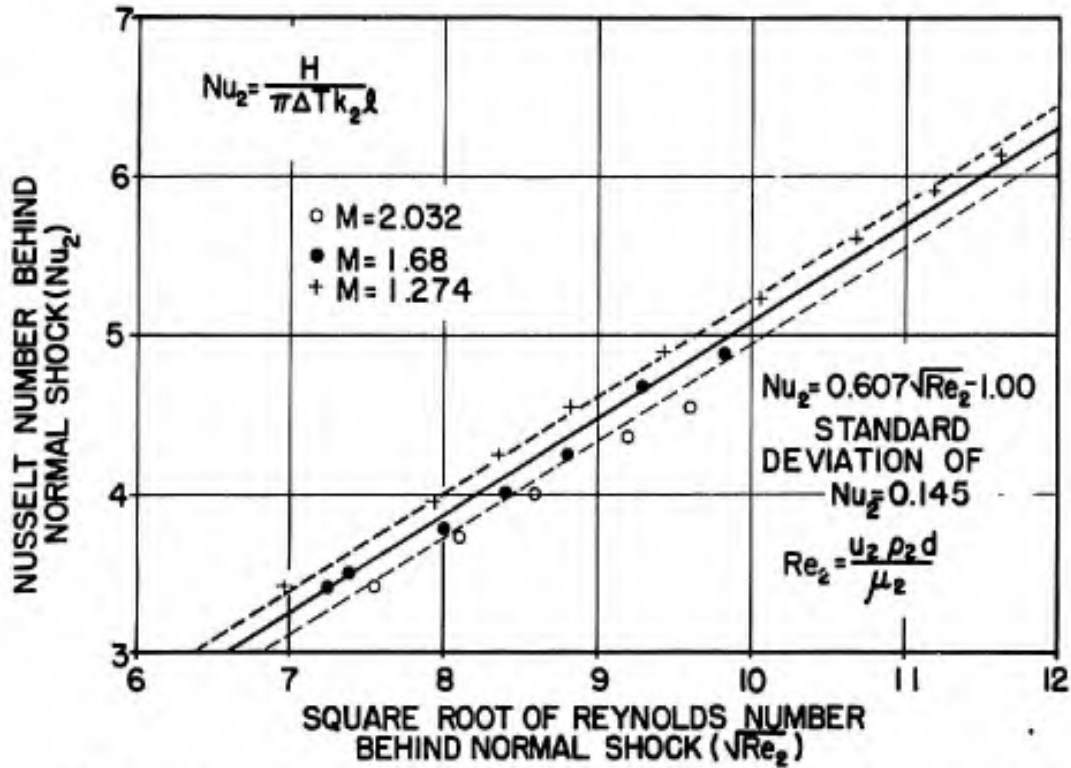


Fig. 13 HEAT LOSS IN WIRE AT SUPERSONIC SPEEDS  
WIRE DIAMETER 0.00015 INCH

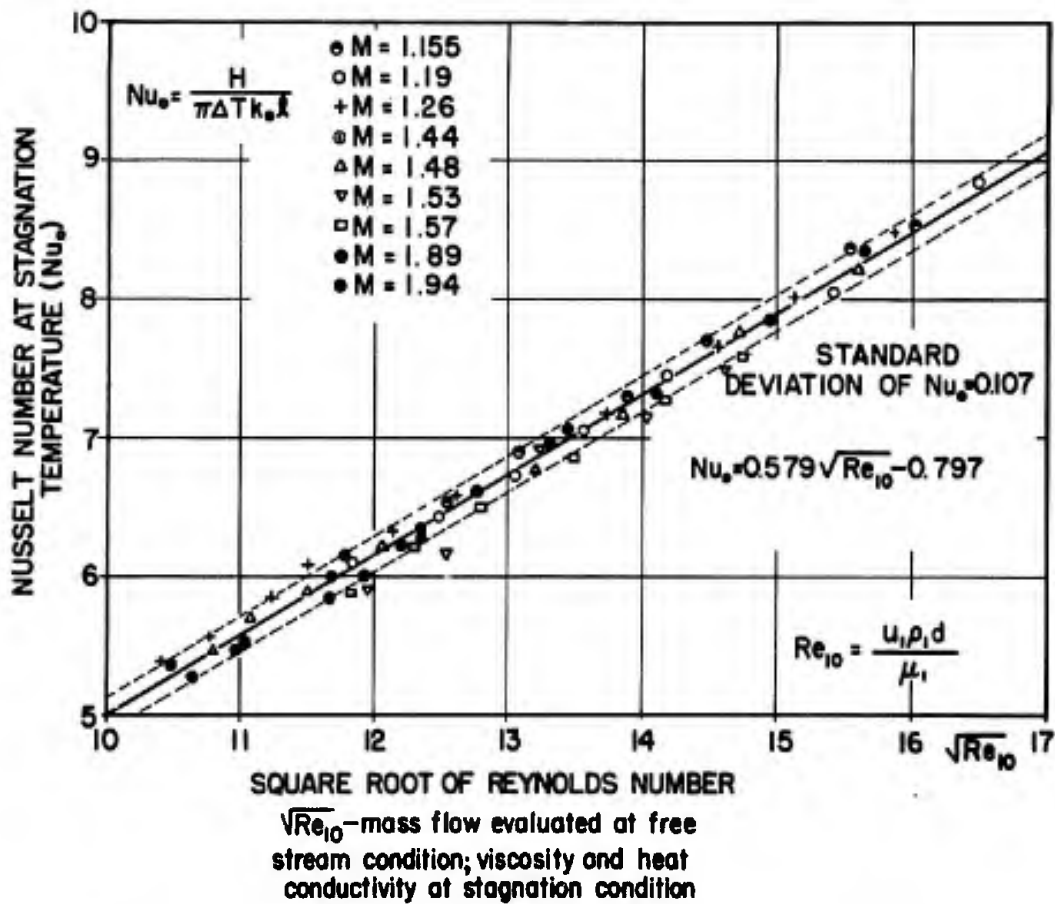


Fig. 14 HEAT LOSS IN WIRE AT SUPERSONIC SPEEDS  
WIRE DIAMETER 0.0003 INCH

of supersonic Mach numbers. When the results were applied to the deduction of a method for the measurement of turbulent fluctuations, it appeared that the use of stagnation temperature, viscosity, and heat conduction would be preferable, and we tried to investigate how much error occurs by replacing  $k_2$  by  $k_0$  and  $\mu_2$  by  $\mu_0$ .

It can be seen in Fig. 11 that the temperature behind normal shock is not very far from stagnation temperature, and an estimate shows that the spread due to this rearrangement cannot increase more than 3 to 4 per cent. Since, from continuity  $\rho_1 U_1 = \rho_2 U_2$ , the new parameters are

$$Nu_0 = \frac{H}{L \pi \Delta T k_0} \quad (4) \quad \text{and} \quad Re_{10} = \frac{U_1 \rho_1 d}{\mu_0} \quad (5)$$

The subscript 10 refers to the fact that the mass flow is evaluated at condition 1, and the viscosity at stagnation condition.

The same data replotted with these parameters is shown in Fig. 14, 15, and 16. The resulting scatter is reduced and the two sets of data fit together reasonably well.

This fact establishes an empirical law for the heat loss at low temperature loadings for infinitely long wire for the air

$$\frac{H}{L \pi \Delta T k_0} = 0.58 \sqrt{\frac{U_1 \rho_1 d}{\mu_0}} - 0.795 \quad (6)$$

The negative intercept is different from the low speed data, but we believe that it has no fundamental significance, since the law is not expected to hold at very low Reynolds numbers. The lower part of the line is practically in the slip-flow region and slip-flow effect would invalidate these findings at Reynolds numbers near unity.

The third problem was the determination of the effect of large temperature loadings. This was the most difficult part of the program, since the number of wire failures increased rapidly with increased operating temperatures. Again, the criterion of determining whether or not a wire had been permanently impaired, was the drift in cold resistance during the run. Useful data were obtained with temperatures as high as 300 degrees centigrade.

The results can be expressed in the following manner: if we expand the heat loss in a power series in terms of the temperature loading at fixed M and Re, we get

$$H(\tau) = \left( \frac{\partial H}{\partial \tau} \right)_{\tau=0} \tau + \frac{1}{2} \left( \frac{\partial^2 H}{\partial \tau^2} \right)_{\tau=0} \tau^2 + \dots$$

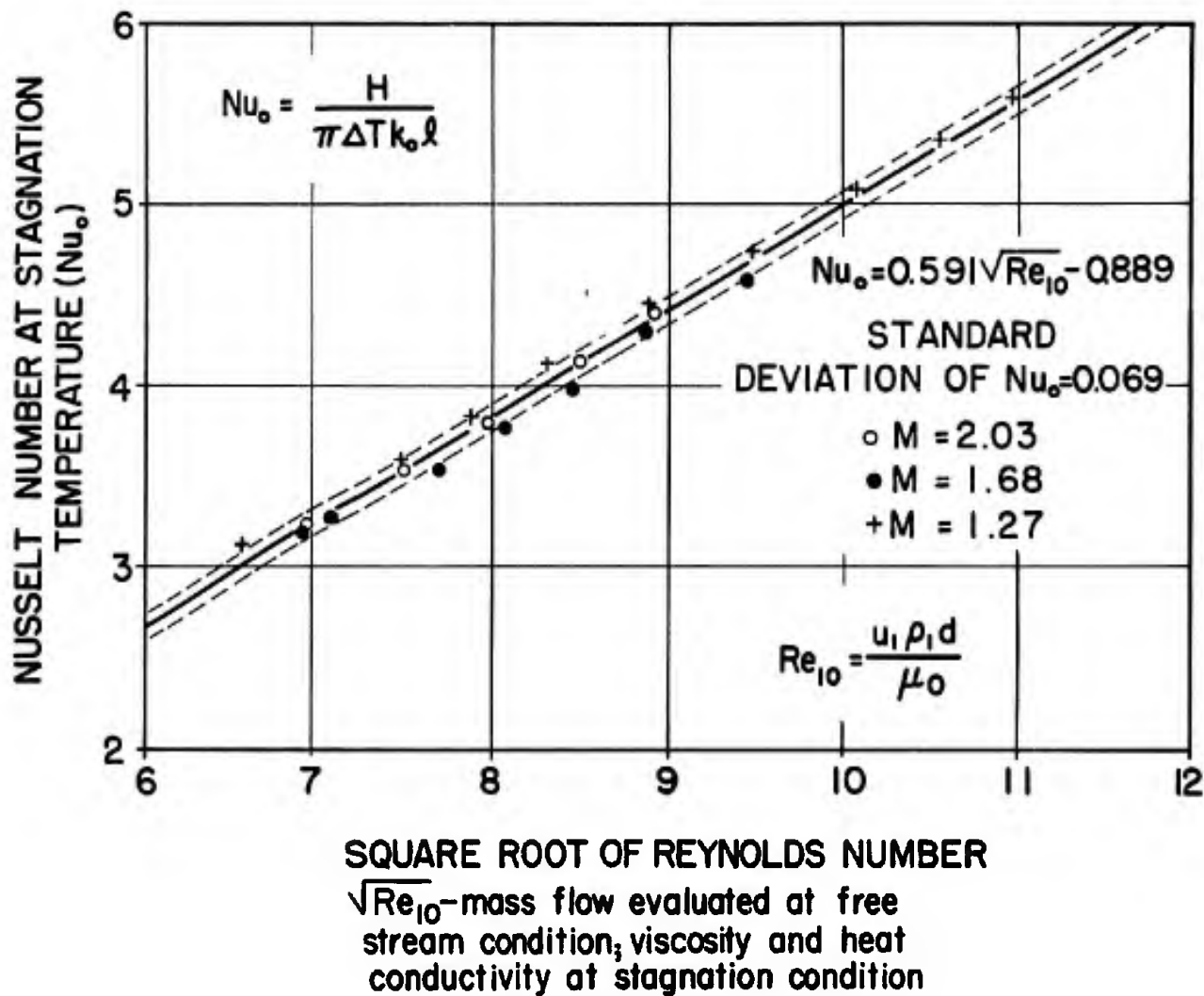
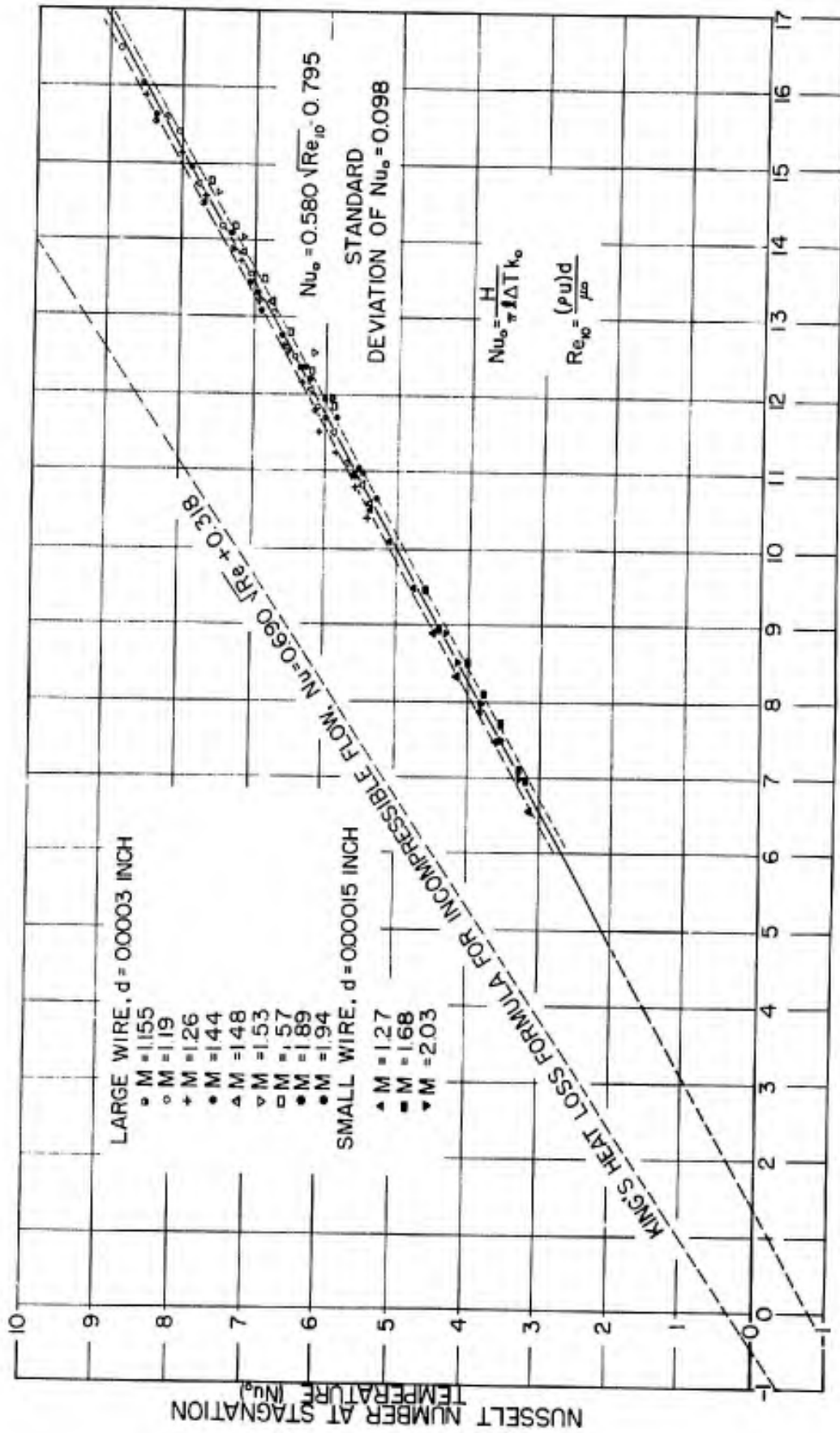


Fig. 15 HEAT LOSS IN WIRE AT SUPERSONIC SPEEDS  
 WIRE DIAMETER 0.00015 INCH



SQUARE ROOT OF REYNOLDS NUMBER

$\sqrt{Re_{10}}$ -mass flow evaluated at free stream condition; viscosity and heat conductivity at stagnation condition

Fig. 16 HEAT LOSS OF WIRE AT SUPERSONIC SPEEDS - LARGE AND SMALL WIRE

Keeping only the first two terms,

$$H(\tau) = \left( \frac{\partial H}{\partial \tau} \right)_{\tau=0} \tau [1 - C\tau]$$

where

$$C = -\frac{1}{2} \frac{\left( \frac{\partial^2 H}{\partial \tau^2} \right)_{\tau=0}}{\left( \frac{\partial H}{\partial \tau} \right)_{\tau=0}}$$

The Nusselt number becomes

$$Nu(\tau) = [Nu]_{\tau=0} [1 - C\tau] \quad (7)$$

The value of heat loss for small temperature loading gives the value of  $\left( \frac{\partial H}{\partial \tau} \right)_{\tau=0}$ , and for every M and Re the plot,  $H = H(\tau)$ , was obtained.

It was found early in the research that the heat loss is nonlinear with  $\tau$ , i.e., as it falls off below the linear relationship as shown in Fig. 17. This was rather surprising as either radiation effects or the increased conductivity at higher temperatures would suggest an upward trend.

The only rational explanation that we can offer is that the added heat "blows" the normal shock forward and thus decreases the temperature gradients. When the value of C was determined from the measurements, it was found that it was practically independent of both Reynolds and Mach numbers and had an approximate value of 0.18. Since the experimental determination of a second order effect is rather difficult, the scattering of results is great. (The standard deviation of the value of C was 20 per cent.) It did not show any systematic variation with either M or Re.

Since our primary interest was to find the functional form of the supersonic heat loss in order to determine the fluctuation of a supersonic hot-wire anemometer, the investigations were terminated at this level. We felt that further refinement would lead to diminishing returns; the accuracy could not be expected to improve much, due to inherent limitations in the experimental set-up. The empirical form of the heat loss law can be found from combining equations 6 and 7:

$$H = \pi d k_0 [T_w - T_e] \left[ A \sqrt{\frac{U_1 \rho_1 d}{\mu_0}} - B \right] \left[ 1 - C \frac{T_w - T_e}{T_0} \right] \quad (8)$$

where the region explored was

$$30 < \frac{U_1 \rho_1 d}{\mu_0} < 400 \quad 300^\circ\text{K} < T_w < 650^\circ\text{K}$$

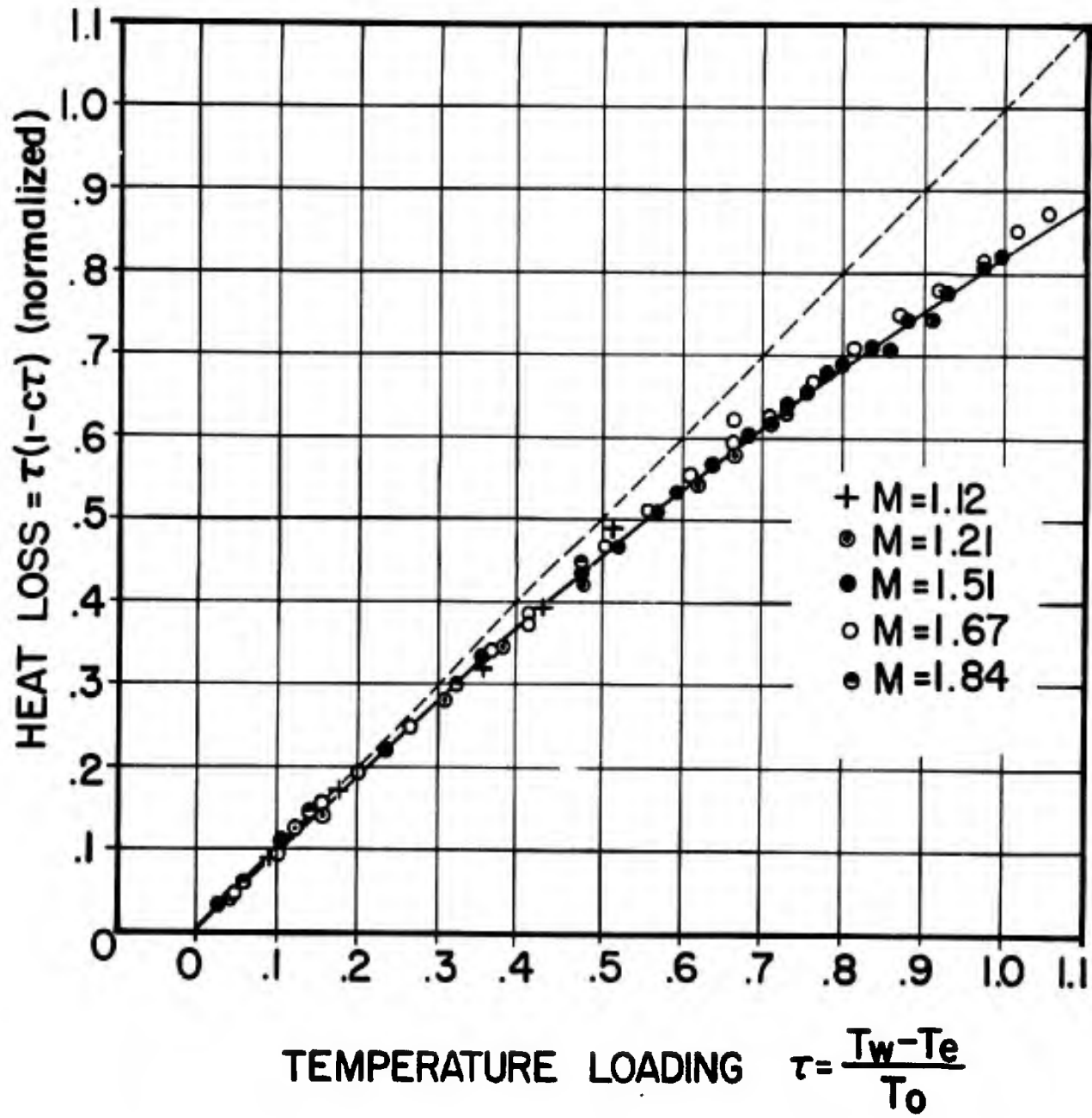


Fig. 17 HEAT LOSS VS TEMPERATURE LOADING

The constants A, B, C for infinitely long wires:

$$A = 0.580$$

$$B = 0.795$$

$$C = 0.180$$

#### COMPARISON WITH EXISTING THEORY

Tsien and Finston gave an approximation to the heat loss of hot wires in compressible flow in a report on November 28, 1948.<sup>10</sup> They assumed  $Pr = 1$ , no shock, and represented the hot-wire by a flat ribbon of width  $L$  parallel to the flow. The heat loss of one side of the ribbon is given in equation 5 of the report and, in present notation, is repeated here:

$$H/L = 0.664 k_w T_1 \sqrt{\frac{U_1 \rho_1 L}{\mu_1}} \frac{\mu_1}{\mu_w} \left[ \left( \frac{T_w}{T_1} - 1 \right) - \frac{\gamma-1}{2} M^2 \right] \quad (9)$$

Doubling to account for both sides of the strip, and using the relations

$$\frac{T_0}{T_1} = 1 + \frac{\gamma-1}{2} M^2 \quad ; \quad \frac{\mu_1}{\mu_w} = \frac{k_1}{k_w}$$

Tsien's and Finston's formula becomes

$$H = 1.328 k_0 \ell \frac{U_1 \rho_1 L}{\mu_0} (T_w - T_0) f(M) \quad (10)$$

Clearly, that  $T_e = T_0$  in their case is plausible from the assumption that  $Pr = 1$ . The Nusselt number becomes

$$Nu_0 = \bar{A} \sqrt{Re_{10}} f(M) \quad (11)$$

where  $Nu_0$  and  $Re$  have the same definition as in equations 4, 5, 6, and  $f(M)$  is a function of Mach number given below.

The formula for the Nusselt number they obtained has three distinctive features:

1. Describes linear dependence with the square root of Reynolds number for a fixed Mach number, and gives strict linearity with temperature difference between wire and air.
2. Does not describe intersection with the  $Nu$  axis as found in experiments.
3. Has a Mach number dependence  $f(M)$  not shown in our experiments.

---

<sup>10</sup> "Hot-Wire Anemometer in High Speed Flows," Tsien and Finston, Meteor Report, Nov. 28, 1948

TABLE

| <u>M</u> | <u>f(M)</u> |
|----------|-------------|
| 0        | 1.00        |
| .5       | .98         |
| 1.0      | .93         |
| 1.5      | .87         |
| 2.0      | .80         |
| 2.5      | .73         |
| 3.0      | .67         |
| 5.0      | .50         |
| $\infty$ | 0           |

The table indicates that the difference between  $M = 1$  and  $M = 2$  amounts to 13 to 14 per cent. Obviously, this results from neglecting the shock wave, which apparently plays an important role in the case of a cylinder, perhaps more important than in the case of a flat ribbon.

#### CONCLUDING REMARKS

The purpose of this investigation was to determine the heat loss from hot-wires in supersonic flow in order to provide a basis for determination of the fluctuation sensitivity of the wires for turbulence measurements.

Other aspects of the supersonic hot-wire anemometer were given by the senior author in a paper presented to the IAS on January 29, 1950.<sup>11</sup> The conclusion of the investigations on the fluctuation sensitivity is that the wire is sensitive to stagnation temperature fluctuations and mass flow fluctuations in varying degrees, depending on the wire operating temperature. This means that by varying the wire operating temperature the two kind of fluctuations can be separated. This fact gave impetus to the determination of nonlinear effects at high temperature loading.

---

<sup>11</sup> "The Hot-Wire Anemometer in Supersonic Flow," L.S.G. Kovásznay, Paper presented at the 18th Annual Meeting of the IAS, January 29, 1950.

## NOTATION

### Subscripts denote:

|              |                               |
|--------------|-------------------------------|
| $e$          | at equilibrium temperature    |
| $r$          | at reference temperature      |
| $w$          | at wire temperature           |
| $0$          | at stagnation temperature     |
| $1$          | free stream condition         |
| $2$          | condition behind normal shock |
| —            | mean (time average)           |
| no subscript | "in general"                  |

---

|            |   |
|------------|---|
| $a_w$      | overheating ratio                                 |
| $\alpha$   | temperature coefficient of electrical resistivity |
| $T$        | temperature                                       |
| $\Delta T$ | $T_w - T_e$                                       |
| $\tau$     | Temperature loading factor                        |
| $\sigma_T$ | maximum tensile stress                            |
| $r$        | specific electric resistivity of wire             |
| $d$        | diameter of the wire                              |
| $l$        | length of the wire                                |
| $c$        | speed of sound                                    |
| $U$        | velocity  |
| $\rho$     | density   |
| $p$        | pressure  |
| $\mu$      | viscosity   |
| $K$        | heat conductivity of the wire                     |
| $k$        | heat conductivity of the air                      |
| $C_p$      | specific heat at constant pressure                |
| $\gamma$   | $C_p/C_v$ ratio of specific heats                 |

|                          |   |
|--------------------------|---|
| <b>M</b>                 | <b>Mach number</b>  |
| <b>Pr</b>                | <b>Prandtl number</b>   |
| <b>Re</b>                | <b>Reynolds number</b>  |
| <b>Re<sub>10</sub></b>   | <b>Reynolds number when the mass flow is evaluated at free stream condition and the viscosity and heat conductivity at stagnation condition</b> |
| <b>H</b>                 | <b>Heat loss of the wire per unit time</b>  |
| <b>H<sub>corr</sub></b>  | <b>correct value of heat loss</b>   |
| <b>H<sub>meas</sub></b>  | <b>measured value of heat loss</b>  |
| <b>Nu</b>                | <b>Nusselt number</b>   |
| <b>Nu<sub>corr</sub></b> | <b>correct value of Nusselt number for infinitely long wire</b>   |
|                          | $\text{Nu}_{\text{corr}} = \frac{H_{\text{corr}}}{\pi L \Delta T k_0}$  |
| <b>Nu<sub>meas</sub></b> | <b>measured Nusselt number on a finite wire</b>   |
|                          | $\text{Nu}_{\text{meas}} = \frac{H_{\text{meas}}}{\pi L \Delta T k_0}$  |
| <b>S</b>                 | <b>non-dimensional parameter for end loss correction</b>  |
| <b>A, B, C</b>           | <b>non-dimensional constants</b>  |
| <b>L</b>                 | <b>flat ribbon width</b>  |

---